Orthonormal Polynomial Bases for Airfoil Design

Dan Berkenstock
Dept. of Aeronautics and Astronautics
Stanford University
496 Lomita Mall
Stanford, CA 94305
dberkens@stanford.edu

Juan Alonso
Dept. of Aeronautics and Astronautics
Stanford University
496 Lomita Mall
Stanford, CA 94305
jjalonso@stanford.edu

Laurent Lessard
Dept. of Mechanical and Industrial Engineering
Northeastern University
360 Huntington Avenue
Boston, MA 02115
l.lessard@northeastern.edu

***Abstract*—Shape parameterization plays an important role in the process of Aerodynamic Shape Optimization (ASO). A good parameterization allows the optimizer to easily explore the design space at multiple scales, while not adversely affecting the convergence or accuracy of the solution. Over the last several decades, a wide variety of methods have been proposed and characterized for representing aerodynamic shapes, including various polynomial representations, classes of splines, and radial basis functions. Our research into the application of convex optimization techniques to aerospace design has motivated us to revisit and expand these techniques, particularly for those with convex representations. For such parameterizations, when coupled with convex objective functions and constraints, convergence is guaranteed to globally optimal solutions in polynomial time. This guarantee allows for comparison of the results obtained with different shape representations without potentially adverse complications related to selection of initial conditions, local optima, or noisy gradients. In the course of this work we make several contributions. First, we provide orthonormal extensions to several common polynomial bases. Second, we demonstrate efficient objective function representation for supersonic drag minimization problems when employing an integral form of such orthonormal bases. Finally, we develop an analytic solution to a sample benchmark problem and compare the solutions offered by a finite linear combination of design variables with basis functions, to the underlying continuous result.**

TABLE OF CONTENTS

1. INTRODUCTION

In this paper, we explore several polynomial bases for representing airfoils and compare the efficacy of those representations by solving a benchhmark convex optimization problem with each. We refer the reader to our previous paper [1] for a general primer on convex optimization and its applicability to Aerodynamic Shape Optimization (ASO) as well as background references.

As a core concept of this research, we continue to explore the benefits and limitations of casting conceptual airfoil design as a convex optimization problem. A convex optimization problem takes the general form

$$\begin{aligned} \underset{x}{\text{minimize}} \quad & f_0(x) \\ \text{subject to} \quad & f_i(x) \leq 0,\ i = 1, \ldots, m, \end{aligned} \tag{1}$$

where $x \in \mathbb{R}^n$ is a vector of design variables and the $f_i : \mathbb{R}^n \to \mathbb{R}$ are convex objective and constraint functions. A function $f : \mathbb{R}^n \to \mathbb{R}$ is convex if the domain of f is a convex set and if for all $x, y \in \operatorname{dom} \mathrm{f}$, with $0 \leq \theta \leq 1$,

$$f(\theta x + (1-\theta)y) \leq \theta f(x) + (1-\theta) f(y). \tag{2}$$

For a comprehensive review of convex optimization and convex functions we refer the reader to Boyd and Vandenberghe [2]. A list of common convex functions and their domains is included in Table 1.

Function	Domain	Curvature
Summation	$X \in \mathbb{R}^{m \times n}$	convex
Max	$X \in \mathbb{R}^{m \times n}$	convex
Min	$X \in \mathbb{R}^{m \times n}$	concave
2-norm	$x \in \mathbb{R}^n$	convex
PSD quadratic form	$x \in \mathbb{R}^n$, $P \succeq 0$	convex
Quadratic over linear	$x \in \mathbb{R}^n$, $y > 0$	convex
Inverse positive	$x > 0$	convex

Table 1. Representative convex functions

There is a rich body of previous work describing different approaches to airfoil representation for shape design. For example, Song and Keane [3], Masters et al. [4], and Sripawadkul, Padulo, and Guenov [5] all provide excellent overviews of shape paramerization techniques for aerospace shape optimization, including the use of splines. The well-known Class-Shape-Transformation (CST) method [6–8] for shape parameterization employs Bernstein polynomials. In [9], Rajnarayan et al describe a universal shape parameterization for airfoils using B-splines. Also, in [10], Li and Krist discuss the benefits of incorporating curvature-based smoothing techniques in the optimization of transonic airfoils. In general, the use of various types of splines, including surface and volumetric, has been well studied in the design of airfoils and more general aerodynamic shapes.

In this paper, we make several contributions. First, we review three traditional polynomial bases for aerospace design.

Second, we develop a set of orthonomal bases by applying Modified Gram-Schmidt orthogonalization to these original bases. Next, we propose new bases that generalize the previous ones. Then, we derive convex expressions of drag, using supersonic small disturbance theory, and angle of zero lift, using subsonic thin airfoil theory, for a general polynomial basis and apply them to the bases under consideration. Finally, we derive a calculus of variations problem to solve for an optimal shape, in the continuous sense, and compare the resulting discretized solutions obtained using the various approaches.

2. POLYNOMIAL BASES

In this work, we will consider *polynomial airfoils*, which are airfoils defined by separate polynomials representing the upper and lower surfaces,

$$\begin{aligned} y_u(x) &= \sum_{k=0}^{n} a_k P_k(x) \\ y_l(x) &= \sum_{k=0}^{n} b_k P_k(x), \end{aligned} \tag{3}$$

where y_u and y_l represent the upper and lower surfaces, respectively, a and b are linear vectors of design coefficients, and P_k are basis functions that are defined over the range $0 \leq x \leq 1$. Note, that in this case we assume a chord length of unity. Our approach is general and can be used with polynomials of arbitrary degree. Of particular interest is the fact that, regardless of the convexity of the set enclosed by the shape, these representations of the airfoil surface are convex functions with respect to arbitrary a and b. This is in contrast to other shape representations, such as non-uniform rational b-splines (NURBS), where there may be separate vectors of design coefficients, knot coefficients, and weighting coefficients. The fact that these polynomial representations are convex, *with respect to their coefficients*, allows for their inclusion in convex optimization problems. It is important to note, and perhaps somewhat counterintuitive, that the actual set described by these curves, the airfoil, may not itself be a convex shape, though its functional representation is, with respect to the coefficients that will form the vector of design variables in subsequent optimization problems. Additionally, the camberline and thickness profile of the airfoil are also polynomial functions, which are convex with respect to the design coefficients,

$$\begin{aligned} y_c(x) &= \frac{1}{2}\left(y_u(x) + y_l(x)\right) \\ y_t(x) &= \frac{1}{2}\left(y_u(x) - y_l(x)\right). \end{aligned} \tag{4}$$

There is a rich diversity of polynomial bases to select from to represent P_k, from the standard monomial basis, to orthogonal polynomials such as those derived by Legendre and Chebyshev, to power function bases with noninteger powers.

There are important considerations in aerospace design that differ from the design of other shapes. First, airfoils are typically defined over the range $0 \leq x \leq 1$, assuming a chord length of unity. Second, at least for airfoils which will operate partially in subsonic flows, it is typical for the leading and trailing edges to meet, such that $y_u(0) = y_u(1) = y_l(0) = y_l(1) = 0$. Finally, there is often a desire to enable an infinite, or nearly infinite, slope at the leading edge in order to admit the types of rounded nose shapes that are consistent with the NACA 4, 5, & 6 digit airfoils, as well as most, subsonic airfoils.

Common Polynomial Bases for Aerospace Design

Several commonly employed polynomial bases are described below, including the standard monomial basis, the Legendre plus square root basis, and the Component Shape Transform (CST) basis.

Standard Monomial Basis—The simplest polynomial basis is the standard monomial basis, where,

$$P_k = x^k. \tag{5}$$

This is an extremely simple basis to implement programmatically. It also has the benefit that the leading edge and trailing edge conditions can be modeled as,

$$\begin{aligned} y_u(0) &= a_0 = 0 \\ y_u(1) &= \sum_{k=0}^{n} a_k = 0. \end{aligned} \tag{6}$$

Legendre Plus Square Root Basis—In the early literature on shape optimization, Hicks proposed using a combined basis of the Legendre polynomials plus an additional square root term [8, 25]. This is shown below with P_k, $k \geq 1$, given by the Rodrigues formula.

$$\begin{aligned} P_0 &= \sqrt{x} \\ P_k &= \frac{1}{2^{k-1}(k-1)!}\frac{\mathrm{d}^{k-1}}{\mathrm{d}x^{k-1}}(x^2-1)^{k-1}. \end{aligned} \tag{7}$$

Although this basis cannot exactly describe a conic section [11], the square root term allows for the leading edge infinite slope that is necessary to model the type of blunt leading edge exhibited in NACA style subsonic and moderately supersonic airfoils.

However, we note that the point of this term is the ability to approach an infinite slope at the origin, and the square root is only one potential choice. In fact, the square root term complicates further aerodynamic analysis in the following way. Several analytic results, including supersonic small disturbance theory, include integrals of the type,

$$J = \int_{x_1}^{x_2} \left(\frac{\mathrm{d}y}{\mathrm{d}x}\right)^2 \mathrm{d}x, \tag{8}$$

where J is a figure of merit, y is the function describing the curve, and $[x_1, x_2]$ is the interval over which the shape is defined. In the case of an airfoil, $x_1 = 0$, which will lead to an undefined result for this integral. In order to overcome this limitation, we note that,

$$J = \int_0^1 \left[\frac{\mathrm{d}}{\mathrm{d}x}(x^p)\right]^2 \mathrm{d}x, \tag{9}$$

is convergent for $p > 1/2$. However, it is divergent for $p = 1/2$.

Component Shape Transform (CST) Basis—The Component Shape Transform (CST) basis is a popular and flexible strategy for modeling aerodynamic shapes proposed by Brenda

Kulfan [8]. Prototypical airfoil-like shapes are modeled by multiplying a component class, $x^{n_1}(1-x)^{n_2}$, by a shape transformation specified as the inner product of a vector of linear design variables with the vector of Bernstein polynomials of given degree, so that, for a standard airfoil shape,

$$P_k^n(x) = x^{1/2}(1-x)\binom{n}{k}x^k(1-x)^{n-k}. \tag{10}$$

In subsequent sections we employ the Bernstein basis, without the leading terms, in order to maintain a consistent maximum degree across polynomial bases. The ultimate solutions are not impacted as it is straightforward to constrain the leading and trailing edges using our optimization approach.

Orthogonalization

Orthogonal polynomials differ from standard polynomials in that the various P_k are said to be orthogonal, meaning that,

$$\int_{x_1}^{x_2} P_k(x)P_j(x)w(x)\mathrm{d}x = C_k\delta_{kj}, \tag{11}$$

where δ_{kj} is the Kronecker delta function, which is equal to one if $k = j$ and is equal to zero otherwise. C_k is a constant representing the integral of $P_k^2 w(x)$ over the domain. x_1 and x_2 express the limits over which orthogonality is desired and $w(x)$ is a weighting function. A basis is said to be orthonormal if each term of the basis is normalized such at $C_k = 1$.

Orthogonalization and normalization potentially provide several attractive benefits for numerical optimization, including lower condition number of quadratic forms, increased numerical stability, and, in some cases, simpler expression of objective functions and constraints. At least in the geometric sense, an orthogonal basis of design variables should exhibit less correlation between individual variables, and therefore, is likely to converge in fewer iterations.

Creating an orthogonal basis is completed using Modified Gram-Schmidt orthogonalization. As described by Golub [12], the process starts with an input vector of monomials, $\vec{v}$, or other power functions, and defining an inner product as,

$$\langle P_i, P_j\rangle = \int_{x_1}^{x_2} P_i(x)P_j(x)w(x)\,\mathrm{d}x. \tag{12}$$

The first term of the unnormalized basis, $\tilde{P}_0$, is

$$\tilde{P}_0 = v_0. \tag{13}$$

The normalized basis function, P_0, is

$$P_0 = \frac{\tilde{P}_0}{\sqrt{\langle \tilde{P}_0, \tilde{P}_0\rangle}}. \tag{14}$$

The subsequent basis functions are defined by recursion,

$$\tilde{P}_i = v_i(x) - \sum_{j=0}^{i-1}\langle v_i(x), P_j(x)\rangle P_j(x), \tag{15}$$

and, similarly,

$$P_i = \frac{\tilde{P}_i}{\sqrt{\langle \tilde{P}_i, \tilde{P}_i\rangle}}. \tag{16}$$

Convex Orthonormal Bases for Aerospace Design

In aerospace shape optimization, there competing drivers in selection of a shape parameterization. In general, aerodynamic shapes tend to be smooth, in order to reduce the likelihood of flow separation, and concurrent increased drag. Airfoils also tend to exhibit limited variation of curvature, or high frequency oscillations over the surface. In the case of traditional, gradient-based, optimization where local minima are highly likely, it is important to have a basis that easily approximates shapes in the neighborhood of the design space where a global optimum is expected. That is one reason for the popularity of the CST method, the first mode of the basis closely resembles a common airfoil shape and the higher order modes are responsible for variations on that basic theme. In the case of convex optimization, the optimizer is guaranteed to find a global optimum. Therefore, there is less priority on retaining modes that mimic an expected final shape and more priority on having a basis that enables simple derivation of the objective function and constraints, and will lend itself to fewer iterations to convergence.

The discussion of the previous section suggests that orthonormal bases would be good candidates for these problems. However, this does not appear to be an area that has been generally explored, at least in the recent past. Although Bernstein polynomials exhibit several attractive qualities, they are not orthogonal. Similarly, although the orthogonal Legendre polynomials have been used in aerospace shape optimization, when an additional square root term is added, that orthogonality is lost.

In order to investigate and expand the set of known polynomial bases at the disposal of designers, we propose a general category of polynomial basis functions that we call Convex Orthonormal Bases for Aerospace Design (COBAD).

In general, this family of functional bases share several common attributes helpful for aerospace shape optimization problems:

1. The bases are orthonormal over the domain $0 \le x \le 1$.

2. The bases easily admit solutions that close at the leading and trailing edges.

3. The bases support common aerospace objective function evaluation while avoiding divergent integrals.

Some of the bases are already well known, such as that of Legendre, however we extend them by showing how using an integral form can dramatically simplify certain drag minimization problems.

In the remainder of this section, we derive a cross section of COBAD basis functions.

Shifted Legendre Polynomials— For the shifted Legendre polynomials, the input vector is the standard monomial vector, but integrated over the range $x_1 = 0,\ x_2 = 1$, versus the standard definition for the Legendre polynomials where $x_1 = -1$, $x_2 = 1$. The input vector is $\vec{v} = [1,\ x,\ x^2,\ \ldots,\ x^n]$.

Following this approach, the first several terms of the orhtonormalized basis are as shown below in Figure 2.

The integral form, Shifted Legendre (ON/INT), is calculated via the indefinite integral,

i	$v(i)$	P_i
0	1	1
1	x	$\sqrt{3}\left(-1+2x\right)$
2	x^2	$\sqrt{5}\left(1-6x+6x^2\right)$
3	x^3	$\sqrt{7}\left(-1+12x-30x^2+20x^3\right)$

Table 2. Shifted Legendre (ON) basis terms.

$$P_{i_{\text{int}}} = \int_0^x P_i(x)\,\mathrm{d}x. \tag{17}$$

i	$v(i)$	P_i
0	1	1
1	x	$\sqrt{3}\left(-1+x\right)x$
2	x^2	$\sqrt{5}\left(1-3x+2x^2\right)x$
3	x^3	$\sqrt{7}\left(-1+6x-10x^2+5x^3\right)x$

Table 3. Integral Shifted Legendre (ON/INT) basis terms.

Orthogonal Bernstein—In the orthogonalized Bernstein basis, we employ the Bernstein polynomials of a given order as the input vector, so that for the set of polynomials of degree $n = 3$, the basis functions are shown in Table 4. In this case, $v = \left[(1-x)^3,\, 3x(1-x)^2,\, 3x^2(1-x),\, x^3\right]$.

i	P_i
0	$\sqrt{7}(1-3x+3x^2-x^3)$
1	$\sqrt{5}\left(-1+9x-15x^2+7x^3\right)$
2	$\sqrt{3}\left(1-13x+33x^2-21x^3\right)$
3	$-1+15x-45x^2+35x^3$

Table 4. Orthonormalized Bernstein (ON) basis terms, $n = 3$.

i	P_i
0	$\sqrt{7}\frac{x}{4}\left(4-6x+4x^2-x^3\right)$
1	$\sqrt{5}\frac{x}{4}\left(-4+18x-20x^2+7x^3\right)$
2	$\sqrt{3}\frac{x}{4}\left(4-26x+44x^2-21x^3\right)$
3	$\frac{x}{4}\left(-4+30x-60x^2+35x^3\right)$

Table 5. Integral Bernstein (ON/INT) basis terms, $n = 3$.

Orthogonalized Legendre+—The orthogonalized Legendre+ basis adds an additional power function, x^p into the input vector, where $1/2 < p < 1$. This enables the same infinite slope behavior at the leading edge, but without certain integration difficulties.

3. AERODYNAMIC PERFORMANCE

In this section, we describe several classes of aerodynamic objective function that are helpful in the conceptual design of aerodynamic shapes.

Subsonic Thin Airfoil Aerodynamics

Thin-airfoil theory provides closed form analytic solutions for the lift and moment coefficients of a reasonably thin airfoil in a subsonic, invsicid, irrotational, incompressible flow. As

i	$v(i)$	P_i
0	1	1
1	$x^{3/4}$	$\frac{\sqrt{10}}{6}\left(-4+7x^{3/4}\right)$
2	x	$\frac{1}{\sqrt{3}}\left(7-70x^{3/4}+66x\right)$
3	x^2	$\frac{\sqrt{5}}{3}\left(-7+154x^{3/4}-198x+54x^2\right)$

Table 6. Orthogonalized Legendre+ basis (ON) terms, $p = 3/4$.

i	$v(i)$	P_i
0	1	x
1	$x^{3/4}$	$\frac{2\sqrt{10}}{3}x\left(-1+x^{3/4}\right)$
2	x	$\frac{1}{\sqrt{3}}x\left(7-40x^{3/4}+33x\right)$
3	x^2	$\frac{\sqrt{5}}{3}x\left(-7+88x^{3/4}-99x+18x^2\right)$

Table 7. Integral form Legendre+ basis (ON/INT) terms, $p = 3/4$.

presented in [13], the sectional lift and moment coefficients are dependent solely upon the shape of the camber line:

$$y_c(x) = \frac{y_u(x)+y_l(x)}{2} = \frac{1}{2}\sum_{i=1}^{n}(a_i+b_i)P_i(x), \tag{18}$$

and its slope

$$\frac{\mathrm{dy_c}}{\mathrm{dx}} = \frac{1}{2}\sum_{i=1}^{n}(a_i+b_i)\frac{\mathrm{d}P_i(x)}{\mathrm{d}x}. \tag{19}$$

The sectional lift coefficient is $c_l = 2\pi(\alpha-\alpha_{l0})$, where the angle of zero lift is given by,

$$\alpha_{l0} = \frac{2}{\pi}\int_0^\pi \frac{\mathrm{d}y_c}{\mathrm{d}x}\sqrt{\frac{x}{1-x}}\,\mathrm{d}x. \tag{20}$$

Typically, Equation 20 is converted to cosine coordinates, however we prefer to employ the linear formulation as originally derived by Munk [14] for ease of use in a subsequent calculus of variations test case. The angle of zero lift is a useful quantity in the design process because a more negative angle of zero lift indicates higher aerodynamic performance in level flight.

Similarly, the moment coefficient about the aerodynamic center is

$$c_{\mathrm{m_{ac}}} = \int_0^\pi \frac{\mathrm{dy_c}}{\mathrm{d}x}(4x-3)\sqrt{\frac{x}{1-x}}\,\mathrm{d}x. \tag{21}$$

For this subsonic case, and under thin airfoil assumptions, c_l, c_{mac}, and α_{l0} are affine, and therefore convex, functions of the polynomial coefficients a_i and b_i and the angle of attack α.

Supersonic Thin Airfoil Aerodynamics

As presented in [15, 16], under suitable assumptions including small thickness, camber, and angle of attack and sharp leading edges, the lift and drag coefficients of an airfoil in a supersonic flow may be approximated as

$$\begin{aligned} c_l &= \frac{4\alpha}{\sqrt{M^2-1}} \\ c_d &= \frac{4}{\sqrt{M^2-1}}\left(\alpha^2+K_2+K_3\right). \end{aligned} \tag{22}$$

Again assuming a chord length of 1, the K_2 term accounts for wave drag created by the camber line,

$$K_2 = \int_0^1 \left[\frac{\mathrm{d}}{\mathrm{dx}} \left(\frac{y_u(x) + y_l(x)}{2} \right) \right]^2 \mathrm{dx}, \tag{23}$$

and the K_3 term accounts for wave drag generated by the airfoil thickness,

$$K_3 = \int_0^1 \left[\frac{\mathrm{d}}{\mathrm{dx}} \left(\frac{y_u(x) - y_l(x)}{2} \right) \right]^2 \mathrm{dx}. \tag{24}$$

Therefore, the drag coefficient may be represented as a quadratic form in the polynomial coefficients and the angle of attack. Specifically,

$$c_d = \frac{4}{\sqrt{M^2 - 1}} \left(\alpha^2 + v^T Q v \right). \tag{25}$$

In particular,

$$K_2 + K_3 = \int_0^1 \frac{\dot{y}_u^2}{2} \mathrm{d}x + \int_0^1 \frac{\dot{y}_l^2}{2} \mathrm{d}x, \tag{26}$$

which, expanding, leads to,

$$K_2 + K_3 = \frac{1}{2} \int_0^1 \left[\left(\sum_{i=0}^{n} a_i \frac{\mathrm{d}P_i}{\mathrm{d}x} \right)^2 + \left(\sum_{i=0}^{n} b_i \frac{\mathrm{d}P_i}{\mathrm{d}x} \right)^2 \right] \mathrm{d}x. \tag{27}$$

Making use of the identity for the sum of a square, we see that,

$$\begin{aligned} K_2 + K_3 = &\sum_{i=0}^{n} \frac{a_i^2 + b_i^2}{2} \int_0^1 \left(\frac{\mathrm{d}P_i}{\mathrm{d}x} \right)^2 \mathrm{d}x \\ &+ \sum_{i=0}^{n} \sum_{j=0}^{i-1} (a_i a_j + b_i b_j) \int_0^1 \left(\frac{\mathrm{d}P_i}{\mathrm{d}x} \frac{\mathrm{d}P_j}{\mathrm{d}x} \right) \mathrm{d}x. \end{aligned} \tag{28}$$

and, therefore,

$$Q = \frac{1}{2} \begin{bmatrix} \int_0^1 \left(\frac{\mathrm{d}P_0}{\mathrm{d}x} \right)^2 \mathrm{d}x & \dots & \int_0^1 \left(\frac{\mathrm{d}P_0}{\mathrm{d}x} \frac{\mathrm{d}P_n}{\mathrm{d}x} \right) \mathrm{d}x \\ \int_0^1 \left(\frac{\mathrm{d}P_1}{\mathrm{d}x} \frac{\mathrm{d}P_0}{\mathrm{d}x} \right) \mathrm{d}x & \dots & \int_0^1 \left(\frac{\mathrm{d}P_1}{\mathrm{d}x} \frac{\mathrm{d}P_n}{\mathrm{d}x} \right) \mathrm{d}x \\ \vdots & \ddots & \vdots \\ \int_0^1 \left(\frac{\mathrm{d}P_n}{\mathrm{d}x} \frac{\mathrm{d}P_0}{\mathrm{d}x} \right) \mathrm{d}x & \dots & \int_0^1 \left(\frac{\mathrm{d}P_n}{\mathrm{d}x} \right)^2 \mathrm{d}x \end{bmatrix}. \tag{29}$$

It is straightforward to check that all eigenvalues of Q are positive, and so Q is positive definite, and c_d is a convex function of v. For the simple example of the monomials up to degree 3,

$$Q = \begin{bmatrix} 0 & 0 & 0 & 0 \\ 0 & \frac{1}{2} & \frac{1}{2} & \frac{1}{2} \\ 0 & \frac{1}{2} & \frac{2}{3} & \frac{3}{4} \\ 0 & \frac{1}{2} & \frac{3}{4} & \frac{9}{10} \end{bmatrix}, \tag{30}$$

and the eigenvalues are approximately,

$$\lambda = [0.0,\ 0.007,\ 0.162,\ 1.898]. \tag{31}$$

Also, now we see the value in employing an integral form of an orthogonal basis, the matrix Q becomes the identity matrix of given degree. Using such a basis, minimizing supersonic small disturbance wave drag can be accomplished by solving a sum of squares problem, a significant reduction in derivation effort, and a fact that we can not find referenced elsewhere.

4. VARIATIONAL TEST CASE

For each polynomial basis, the underlying function describing the airfoil is discretized in the sense that it is represented by some discrete and finite linear combination of coefficients and basis functions. In order to compare convergence and accuracy of various polynomial basis functions, we compare them against a problem where the continuous extremal function itself is optimized using the calculus of variations [17].

Consider the problem of minimizing the supersonic wave drag of a thin body, modeled using small disturbance theory, subject to constraints on the minimum enclosed area and the subsonic angle of zero lift, as predicted by thin airfoil theory.

In order to simplify the problem, we consider both isoparametric constraints to be active, or equality constraints, enforced using Lagrange multipliers. The camber and thickness profiles are optimized, and further constrained to be zero at the leading and trailing edges.

Mathematically, we seek to minimize the following variational problem,

$$\begin{aligned} \underset{y_c(x), y_t(x), \lambda_0, \lambda_1}{\text{minimize}} \quad & \int_0^1 J(\dot{y}_c(x), y_c, \dot{y}_t(x), y_t, x)\, \mathrm{d}x \\ \text{subject to} \quad & y_c(0) = y_c(1) = 0 \\ & y_t(0) = y_t(1) = 0 \\ & \int_0^1 2 y_t \, \mathrm{d}x = \mathrm{area}_{\mathrm{target}} \\ & \int_0^1 \frac{2}{\pi} \dot{y}_c \sqrt{\frac{x}{1-x}} \, \mathrm{d}x = \alpha_{\mathrm{l0}_{\mathrm{target}}}, \end{aligned} \tag{32}$$

where the functional, J, is

$$\begin{aligned} J = &\frac{4}{\sqrt{M^2 - 1}} \left(\dot{y}_c^2 + \dot{y}_t^2 \right) \\ &+ \lambda_0 \left(2 y_t - \mathrm{area}_{\mathrm{target}} \right) \\ &+ \lambda_1 \left(\frac{2 \dot{y}_c}{\pi} \sqrt{\frac{x}{1-x}} - \alpha_{\mathrm{l0}_{\mathrm{target}}} \right). \end{aligned} \tag{33}$$

Taking the first variation of this problem and setting it to zero results in a system of two, separable, Euler-Lagrange equations,

$$J_{y_c} - \frac{\mathrm{d} J_{\dot{y}_c}}{\mathrm{d}x} = 0 \tag{34a}$$

$$J_{y_t} - \frac{\mathrm{d} J_{\dot{y}_t}}{\mathrm{d}x} = 0. \tag{34b}$$

First, consider the solution of the ordinary differential equation for the camber line, $y_c(x)$,

$$\sqrt{3} \lambda_1 \sqrt{\frac{1-x}{x}} + 8\pi (x-1)^2 \ddot{y}_c = 0. \tag{35}$$

Applying the boundary conditions and solving for the extremal curve,

$$\begin{aligned} \frac{8\pi}{\sqrt{3}\lambda_1} y_c(x) = &\pi(1+x) + 2\sqrt{x(1-x)} \\ &+ 2\mathrm{i} \log\left(\sqrt{\mathrm{x} - 1} - \sqrt{\mathrm{x}} \right). \end{aligned} \tag{36}$$

Unfortunately, attempting to solve for the Lagrange multiplier, λ_1, results in a divergent integral,

$$-\frac{\alpha_{l0_{\text{target}}}}{4\pi\lambda_1} = \int_0^1 \frac{\pi(x-1)x + 2\sqrt{x^3(x-1)}}{(x-1)^2}\,\mathrm{d}x. \quad (37)$$

Therefore, we instead proceed to solve a perturbed version of the initial problem,

$$\begin{aligned} \underset{y_c(x),y_t(x),\lambda_0,\lambda_1}{\text{minimize}} \quad & \int_0^1 J(\dot{y_c}(x), y_c, \dot{y_t}(x), y_t, x)\,\mathrm{d}x \\ \text{subject to} \quad & y_c(0) = y_c(1) = 0 \\ & y_t(0) = y_t(1) = 0 \\ & \int_0^1 2y_t\,\mathrm{d}x = \text{area}_{\text{target}} \\ & \int_0^1 \frac{2}{\pi}\dot{y_c}\sqrt{\frac{x}{1-x+\epsilon}}\,\mathrm{d}x = \alpha_{l0_{\text{target}}}, \end{aligned} \quad (38)$$

where the functional, J, is

$$\begin{aligned} J = & \frac{4}{\sqrt{M^2-1}}\left(\dot{y_c}^2 + \dot{y_t}^2\right) \\ & + \lambda_0\left(2y_t - \text{area}_{\text{target}}\right) \\ & + \lambda_1\left(\frac{2\dot{y_c}}{\pi}\sqrt{\frac{x}{1-x+\epsilon}} - \alpha_{l0_{\text{target}}}\right), \end{aligned} \quad (39)$$

and $0 \leq \epsilon \ll 1$. In this case, we solve the modified Euler Lagrange equation for $y_c(x)$,

$$(1+\epsilon)\sqrt{\frac{3}{x}}\left(\frac{1}{1-x+\epsilon}\right)^{3/2}\lambda_1 + 8\pi\ddot{y_c}(x) = 0, \quad (40)$$

obtaining,

$$\begin{aligned} y_c(x) = & \frac{\sqrt{3}\lambda_1}{4\pi\sqrt{x(1-x+\epsilon)}}\Bigg(x(1-x+\epsilon) \\ & + \left[(1+\epsilon)\cot^{-1}\left(\sqrt{\epsilon}\right) - \sqrt{\epsilon}\right]\sqrt{x^3(1-x+\epsilon)} \\ & - (1+\epsilon)\sqrt{x(1-x+\epsilon)}\sin^{-1}\left(\sqrt{x/(1+\epsilon)}\right)\Bigg). \end{aligned} \quad (41)$$

The solution for the optimal thickness profile is much simpler. The Euler-Lagrange equation for the thickness profile is,

$$2\lambda_0 - \frac{8\ddot{y_t}(x)}{\sqrt{3}} = 0, \quad (42)$$

with the solution, including the boundary conditions $y_t(0) = y_t(1) = 0$,

$$y_t(x) = -\frac{\sqrt{3}\lambda_0}{8}(x - x^2), \quad (43)$$

so that,

$$\lambda_0 = -8\sqrt{3}(\text{area}_{\text{target}}), \quad (44)$$

and,

$$y_t(x) = 3x(1-x)\text{area}_{\text{target}}. \quad (45)$$

5. RESULTS

With the tools developed in previous sections, we now turn our attention towards a numerical experiment to compare the convergence and accuracy of the given methods.

In particular, we seek to generate a minimal, supersonic drag airfoil, subject to a minimum area and subsonic angle of zero lift constraint, as a function of the design coefficients of the various bases. In order to minimize total variation of curvature and minimize the occurrence of large coefficient values, we introduce regularization in both the design coefficients and the integrated variation of curvature, which results in another quadratic form, Q_1.

Mathematically, this problem may be formulated as,

$$\begin{aligned} \underset{\vec{z}}{\text{minimize}} \quad & \frac{4}{\sqrt{M^2-1}} z^T Q z + \epsilon_1 z^T Q_1 z + \epsilon_2 \left\|z\right\|^2 \\ \text{subject to} \quad & \alpha_{l0}^* = \alpha_{l0_{\text{target}}} \quad (46) \\ & \text{area} = \text{area}_{\text{target}} \\ & y_u(0) = y_u(1) \\ & y_t(0) = y_t(1) \\ & \dot{y_c}(1) = \mu. \quad (47) \end{aligned}$$

where, $z = [a, b]$, includes the coefficients of both the upper and lower surfaces and α_{l0}^* indicates the ϵ formulation from the previous section. We formulate and solve this problem using the open source software CXVPY [18–20] and the open source conic solver, SCS [26, 27].

Using the values in Table 8 results in a drag coefficient calculated by the variational method of $c_d = 0.00528$.

Parameter	Value
$\text{area}_{\text{target}}$	0.025
$\alpha_{l0_{\text{target}}}$	$-2.5°$
μ	$-18.7°$
ϵ	0.01
ϵ_1	0.001
ϵ_2	$1e^{-9}$

Table 8. Test Case Parameters

The resulting camberline is,

$$\begin{aligned} y_c(x) = & -0.125 + 0.055x - \frac{0.394x^{3/2}}{\sqrt{101-100x}} \\ & + \frac{0.004\sqrt{-x(-101+100x)}}{1.01-x} \\ & + 0.080\arctan\left(\frac{10\sqrt{x}}{\sqrt{101}-\sqrt{101-100x}}\right). \end{aligned} \quad (48)$$

Similarly, the optimal thickness profile is,

$$y_t(x) = .075x(1-x). \quad (49)$$

Below, we show the convergence rates of various subsets of the initial and orthonormalized bases for this problem. Figure 1 shows the convergence rates using the Legendre family of standard, orthonormal, and integral form basis

functions for varying degree, n. Figure 2 shows the same with the Bernstein family of basis functions.

Figure 3 shows the convex optimizer solution time and how it scales with polynomial basis and order. Finally, Figures 4 - 7, show a comparison of the optimal airfoils achieved using the variational approach as compared to the discretized approach for several of the standard and orthonormalized bases. In general, each of the bases converged to the variational result with a polynomial of degree less than, $n = 10$, with the exception of the straight monomial basis, which indicates it should generally be avoided for shape optimization problems due to slower convergence.

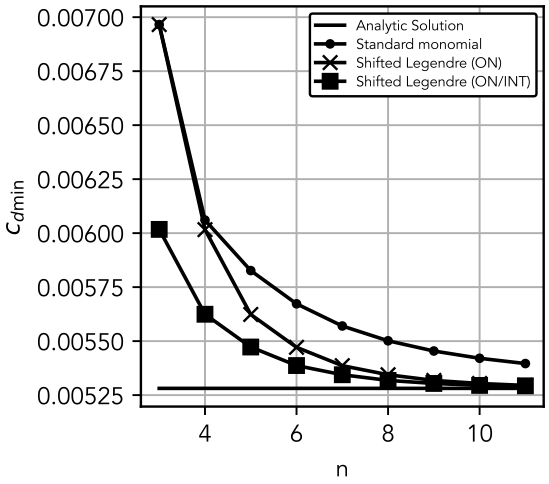

Figure 1. **Comparison of optimal drag coefficients as function of maximum degree of basis (Legendre).**

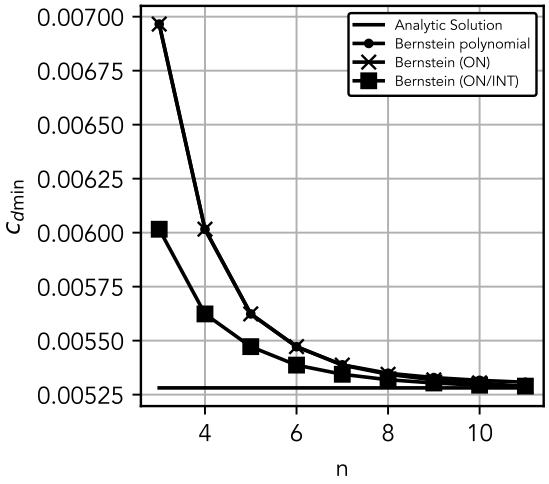

Figure 2. **Comparison of optimal drag coefficients as function of maximum degree of basis (Bernstein).**

6. CONCLUSION

In this paper, we have explored the usage of several orthonormal and orthonormal, integral form polynomial bases for use in convex aerospace shape optimization problems. Initial results indicate that orthonormal bases converge to an analytical result with fewer design variables. In particular, the integral form variations of the orthonormal polynomial bases exhibit the attractive quality that minimizing sum of squares problem, versus a full quadratic form, minimizes the supersonic drag predicted by small disturbance theory. In the future, we plan to extend this analysis to splines and several additional classes of power function based orthonormal bases.

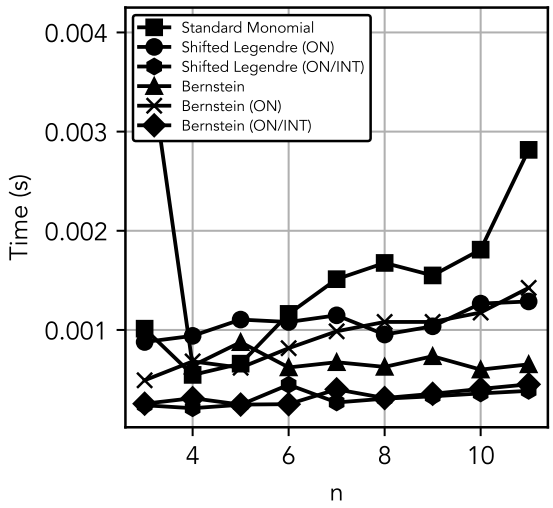

Figure 3. **Solver time for various polynomial bases.**

REFERENCES

[1] Daniel Berkenstock, Juan J. Alonso and Laurent Lessard. "A Convex Optimization Approach to Thin Airfoil Design," AIAA 2022-3356. AIAA AVIATION 2022 Forum. June 2022.

[2] S. Boyd and L. Vandenberghe, Convex Optimization. Cambridge University Press, 2004.

[3] Wenbin Song and Andrew Keane. "A Study of Shape Parameterisation Methods for Airfoil Optimisation," AIAA 2004-4482. 10th AIAA/ISSMO Multidisciplinary Analysis and Optimization Conference. August 2004.

[4] Dominic A. Masters, Nigel J. Taylor, T. Rendall, Christian B. Allen and Daniel J. Poole. "Review of Aerofoil Parameterisation Methods for Aerodynamic Shape Optimisation," AIAA 2015-0761. 53rd AIAA Aerospace Sciences Meeting. January 2015.

[5] Vis Sripawadkul, Mattia Padulo and Marin Guenov. "A Comparison of Airfoil Shape Parameterization Techniques for Early Design Optimization," AIAA 2010-9050. 13th AIAA/ISSMO Multidisciplinary Analysis Optimization Conference. September 2010.

[6] Brenda Kulfan and John Bussoletti. "Fundamental Parameteric Geometry Representations for Aircraft Component Shapes," AIAA 2006-6948. 11th AIAA/ISSMO Multidisciplinary Analysis and Optimization Conference. September 2006.

[7] Brenda M. Kulfan. "Universal Parametric Geometry Representation Method. Journal of Aircraft, 45:1, 142-158, 2008.

[8] Brenda Kulfan. "A Universal Parametric Geometry Representation Method - ĊST;" AIAA 2007-62. 45th AIAA Aerospace Sciences Meeting and Exhibit. January 2007.

[9] Dev Rajnarayan, Andrew Ning and Judd A. Mehr. "Universal Airfoil Parametrization Using B-Splines," AIAA

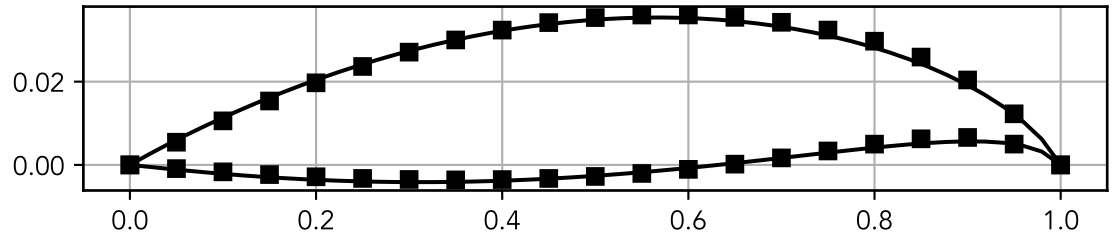

Figure 4. **Optimal variational airfoil (black line) compared against optimal standard monomial airfoil (black squares), $n = 11$.**

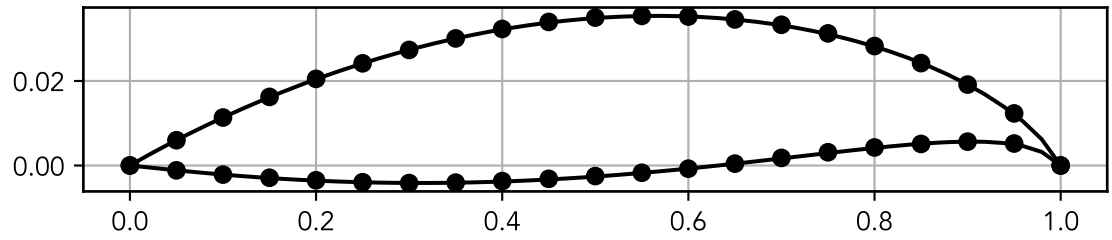

Figure 5. **Optimal variational airfoil (black line) compared against optimal Legendre orthonormal airfoil (black circle), $n = 11$.**

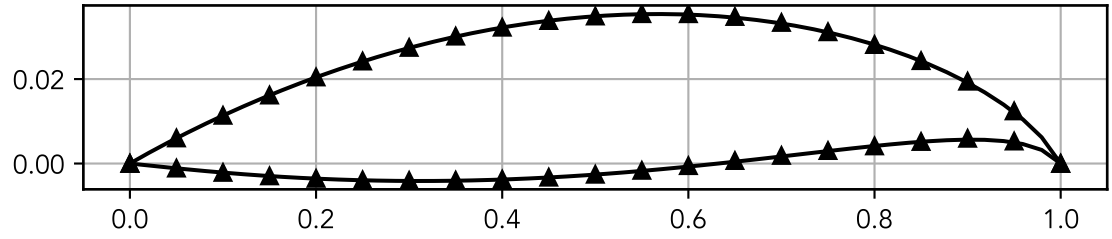

Figure 6. **Optimal variational airfoil (black line) compared against optimal Bernstein polynomial airfoil (black triangle), $n = 11$.**

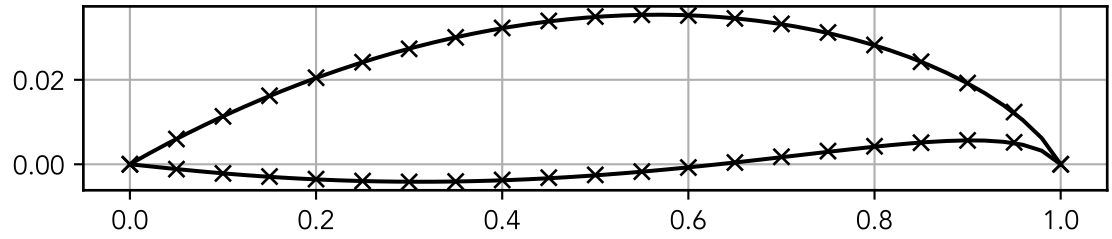

Figure 7. **Optimal variational airfoil (black line) compared against optimal Bernstein orthonormal airfoil (black x), $n = 11$.**

2018-3949. 2018 Applied Aerodynamics Conference. June 2018.

[10] W. Li and S. Krist. "Spline-Based Airfoil Curvature Smoothing and Its Applications." Journal of Aircraft, 42:4, 1065-1074, 2005.

[11] R.C. Beach. "An Introduction to the Curves and Surfaces of Computer-aided Design." Van Nostrand Reinhold. 1991.

[12] Gene H. Golub and Charles Van Loan. "Matrix Computations." The Johns Hopkins University Press. 1996.

[13] J. Moran. "An Introduction to Theoretical and Computational Aerodynamics." Dover Books on Aeronautical Engineering. 2013.

[14] H. Glauert. "The elements of aerfoil and airscrew theory." Cambridge Science Classics, 2nd Edition. 1993.

[15] Arnold M. Kuethe and C.Y. Chow. "Foundations of aerodynamics: Bases of Aerodynamic Design." 3rd Edition. Wiley New York. 1976.

[16] Dan Berkenstock, Juan Alonso and Laurent Lessard. "A Convex Optimization Approach to Thin Airfoil Design." AIAA Aviation Forum. 2022.

[17] Angelo Miele et al. "Theory of Optimum Aerodynamic Shapes." Academic Press, New York. 1965.

[18] S. Diamond and S. Boyd. "CVXPY: A Python-embedded modeling language for convex optimization," Journal of Machine Learning Research, 17(83):1–5, 2016.

[19] A. Agrawal, R. Verschueren, S. Diamond, and S. Boyd. "A rewriting system for convex optimization problems," Journal of Control and Decision, 5(1):42–60, 2018.

[20] Michael Grant, Stephen Boyd, and Yinyu Ye. "Disciplined Convex Programming." In Global Optimization: From Theory to Implementation, edited by Leo Liberti

and Nelson Maculan , 115-210. Springer, New York, NY, 2006.

[21] MOSEK ApS. "MOSEK Optimization Tools Version 10." https://www.mosek.com/products/version-10/. 2023.

[22] Warren Hoburg and Pieter Abbeel. "Geometric Programming for Aircraft Design Optimization," AIAA Journal, 52:11, 2414-2426, 2014.

[23] John D. Anderson, Jr. "Fundamentals of Aerodynamics, 3rd Edition," McGraw-Hill Higher Education, 2001.

[24] Hicks, Raymond M. and Henne, Preston A. . "Wing Design By Numerical Optimization." Journal of Aircraft, 15(7):407-412, 1978.

[25] Hicks, R.M. and Vanderplaats, G.N. . "Application of Numerical Optimization to the Design of Low-speed Airfoils." NASA Technical Memorandum 3213, 1975. National Aeronautics and Space Administration.

[26] O'Donoghue, B., Chu, E., Parikh, N, and Boyd, S. ."Conic Optimization via Operator Splitting and Homogeneous Self-Dual Embedding," Journal of Optimization Theory and Applications, 169:3, 1042-1068, 2016.

[27] O'Donoghue, B. "Operator Splitting for a Homogeneous Embedding of the Linear Complementarity Problem," SIAM Journal on Optimization, 31:3, 1999-2023, 2021.

BIOGRAPHY

Daniel Berkenstock *is a Ph.D candidate in Aeronautics and Astronautics at Stanford, working in the Stanford Aerospace Design Laboratory. Dan received the B.S.E in Aerospace Engineering at the University of Michigan, Ann Arbor, as well as the M.S. in Aeronautics and Astronautics at Stanford University. Dan's research combines the fields of aerospace-focused Multidisciplinary Shape Optimization with Convex Optimization. He has worked previously at Johnson Space Center, Ames Research Center, and Lawrence Livermore National Laboratory and co-founded the satellite imagery provider Skybox Imaging.*

Juan Alonso *is the founder and director of the Stanford Aerospace Design Laboratory (ADL) where he specializes in the development of high-fidelity computational design methodologies to enable the creation of realizable and efficient aerospace systems. His research involves a large number of different manned and unmanned applications including transonic, supersonic, and hypersonic aircraft, helicopters, turbomachinery, and launch and re-entry vehicles. He is the author of over 200 technical publications on the topics of computational aircraft and spacecraft design, multi-disciplinary optimization, fundamental numerical methods, and high-performance parallel computing.*

Laurent Lessard *is an Associate Professor of Mechanical and Industrial Engineering at Northeastern University, with courtesy appointments in ECE and CS. Before joining Northeastern, Laurent was a Charles Ringrose Assistant Professor of Electrical and Computer Engineering at the University of Wisconsin–Madison and a Faculty Member at the Wisconsin Institute for Discovery. Laurent received the B.A.Sc. in Engineering Science from the University of Toronto, and received the M.S. and Ph.D. in Aeronautics and Astronautics at Stanford University, advised by Sanjay Lall and co-advised by Matthew West. His research interests include: decentralized control, robust control, optimization, and machine learning.*